Journal of Testing and Evaluation, Nov. 2004, Vol. 32, No. 6
Paper ID JTE11906
Available online at: www.astm.org

Ashutosh Trivedi[1] *and Sundar Singh*[2]

Cone Resistance of Compacted Ash Fill

ABSTRACT: Coal ash is a granular byproduct of the combustion of coal in coal-fired thermal power plants. The compacted ash is frequently used as a structural fill material. Standard geotechnical investigation methods used for natural soils have revealed inconsistencies when extended to ash fills. The characterization of ash shows morphological dissimilarity with natural soils. It is observed that several groupings of in situ density and stress level lead to similar penetration resistance in coal ash. Thus, the correlations reliable for soils may have questionable interpretations of blow count or measured cone resistance in coal ash. The static cone penetration test results analyzed at various combinations of stress level and relative density indicated the need for a new scheme for interpretation of behavior of ash fills on the basis of relative dilatancy of the ash. The resistance to penetration of the standard cone was interpreted at varying depths on ash fill compacted at varying relative densities. Correlations are suggested to estimate bearing capacity and settlement characteristics of coal ash on the basis of cone penetration test results for direct geotechnical design.

KEYWORDS: coal ash, static cone penetration test, relative density, relative dilatancy, bearing capacity, settlement characteristics.

Introduction

Coal ash is an end product of the combustion of coal and, as such, its composition depends upon the type of coal used in thermal power stations. The rock detritus in the coal varies from one coal sample to another and, therefore, variations are expected among the ashes. In the burning chamber, pulverized coal powder is fired and its subdivision and decomposition occur.

The mineral groups present in coal, such as the hydrated silicate group (kaolin and montmorillonite), the carbonate group (calcite and siderite), the sulfate group (gypsum), and silica (quartz and feldspar), and their varying proportions generally play a major role in determining the chemical composition of the ash. During combustion, as the coal passes through the high temperature zone in the furnace, volatile matter and carbon are burned off while most of the mineral impurities melt. The fused matter is quickly transported to lower temperature zones, where it solidifies as spherical particles of glass. Some of the mineral matter agglomerate forms bottom ash, but most of it flies out with the flue gas stream and is called fly ash. Coal ash is subsequently removed from the gas by electrostatic precipitators (ESPs).

Ropar ash containing less than 10 % lime is normally a product of combustion of anthracite, bituminous, and sub-bituminous coal. In the furnace, when large spheres of molten glass do not get cooled rapidly and uniformly, sillimanite ($Al_2O_3 \cdot SiO_2$) or mullite ($3Al_2O_3 \cdot SiO_2$) crystallize as slender needles in the interior of the glassy spheres. X-ray diffraction of ash has confirmed the presence of quartz, mullite, and hematite or magnetite [1]. These crystalline minerals are nonreactive at ordinary temperatures, and their presence in large proportion tends to reduce reactivity. The absence of peaks associated with hydrated silicates in diffraction analysis of coal ash provides a basis for its treatment as a cohesionless material. The mechanical properties of coal ash depend on the chemical composition, grain size distribution, and density of the deposit. The composition of coal ash depends upon the type of coal used in thermal power stations. The absence of active lime and clay minerals allows coal ash to be considered an inert cohesionless material [1].

The static cone penetration test is a widely used technique to evaluate parameters relevant to geotechnical designs due to its efficacy and reliability. The subsurface explorations turn out to be challenging if the material under investigation is an industrial byproduct, i.e. coal ash, which is a relatively less-investigated geo-material. Several correlations have been suggested in order to obtain soil properties and parameters from the penetration resistance of standard static cones [2].

These approaches have been established for the interpretation of in situ soil parameters but need to be verified for ash by experimental data. The interpretation of cone penetration resistance is normally based on a calibration chamber study that simulates controlled conditions of density and overburden [3]. For cohesive material, the basic soil characteristics can be established from laboratory tests on undisturbed samples, but for cohesionless soils the problem of sample disturbance generally prevents this approach from being used. Therefore, testing under controlled conditions of density and overburden has been developed as the most efficient means of verifying and establishing correlations for cohesionless soils.

Standard cone penetration tests have been carried out on large controlled samples to monitor density, overburden, applied stress, and a constant penetration rate. A large number of standard size reconstituted ash samples have been sheared under drained conditions in a triaxial apparatus to find constitutive relationships for peak friction angle on the basis of knowledge of relative density, mean effective confining pressure, and critical state friction angle.

Review of Previous Work

Coal ash is disposed of hydraulically in the form of slurry in ash ponds constructed near a thermal power plant. These are generally

[1] Professor, Department of Civil Engineering at Delhi College of Engineering, Bawana Road, Delhi 110042, India. E-mail: atrivedi@civil.dce.edu
[2] Formerly Professor, Department of Civil Engineering at Thapar Institute of Engineering & Technology (Deemed University), Patiala 147004, India. E-mail: sundarsingh@mail.tiet.ac.in

TABLE 1—*SPT resistance (N) of ash.*

Investigator	Degree of Compaction	*N*
Cunnigham et al. [4]	95–100 %	10–31
	Loose state	Zero
Dayal et al. [38]	95 %, ash dike	4–27
	Loose state	Zero
Sood et al. [39]	Loose state	Zero–1

loose deposits, which make the fill unstable. Ash dikes restrict the side flow of ash slurry. In order to improve its engineering properties, ash is compacted in layers using vibratory compactors. Standard penetration test (SPT) results on hydraulically deposited ash indicate very low values of *N* (Table 1). The standard penetration test is a widely used technique for soil investigation. It involves the measurement of cutting resistance offered by the soil to the penetration of a standard split spoon barrel, driven by blows from a fixed weight hammer, for 45 cm, out of which the resistance to the first 15 cm of penetration is rejected. The resistance is recorded in terms of the number of blows (*N*) required for 30 cm of penetration at a selected depth (normally at 1.0 or 1.5 m each). It is corrected for various losses besides the corrections for overburden and water table. The relative density obtained from dry densities, determined by a Shelby tube sampler, shows an absence of correlation with the *N*-values for ashes [4]. Toth et al. [5] reported exceptionally wide variation ($N = 10$–55) in standard penetration resistance of Ontario ash, indicating the possibility of presence of the bottom ash.

The static cone penetration test is the next most popular soil investigation technique. This involves continuous measurement of penetration resistance offered to a standard cone by the soils. It has an advantage over the standard penetration test of continuous measurement of the soil resistance. Precisely, the cone resistance obtained in units of pressure is a refinement over the crude measurement of the blow count. The static cone penetration may be idealized as successive and progressive bearing-capacity failure below a small conical footing. Lunne et al [2] discussed this technique in detail that finds application to the investigation on ashes in the present study. Seals et al. [6] reported static cone penetration test (SCPT) results on compacted ash fill where the average friction ratios for ash (3–4.7 %) were appreciably higher than the value (2 %) reported by Schmertmann [7] for clayey silts, sand mixes, silty sands, silts, and fine sands. The graphical relationships proposed by Begemann [8] for the range of average cone resistance and friction resistance values (~1000 and 300 kPa, respectively) indicate a soil type in the range from silty or clayey sand to clayey loam. As per the existing correlations available for natural soils, the predicted range of particles would be 20–60 % finer than silt size, contrary to the 60–80 % actually present.

Therefore, it was understood that the use of Begemann [8] charts might not be extendible to the classification of coal ashes in its totality. Leonards and Bailey [9] suggested that interpretation of load settlement relations for foundation on compacted ash, based on standard penetration tests (SPTs) or static cone penetration tests (SCPTs), may be erroneous because of the inadequacy of these tests to sense the effect of pre-stressing due to compaction.

Interpretation of Cone Penetrometer Bearing Pressure

The static cone penetration resistance may be regarded as the bearing capacity of a small conical footing on a geomaterial. The generally accepted bearing capacity equation for shallow depths uses the bearing capacity factors N_c and N_q proposed by Prandtl [10] and Reisner [11], respectively. However, substantial differences have been reported in the semi-empirical bearing capacity factor for shallow foundations N_γ in numerous studies [12–18].

The classical bearing capacity equation for strip foundations, popularly known as the Terzaghi formula, is given by

$$q_{ult} = c' N_c + \sigma'_{ov} N_q + 0.5 N_\gamma \gamma' B \quad (1)$$

where c' is the effective soil cohesion intercept, σ'_{ov} is the overburden acting at the footing base expressed in terms of effective stress, γ' is the buoyant unit weight, and B is the footing width.

For cohesionless materials the above equation is represented as

$$q_{ult} = \sigma'_{ov} N_q + 0.5 N_\gamma \gamma' B \quad (2)$$

$$N_q = \tan^2(\pi/4 + \phi'/2) e^{\pi \tan \phi'} \quad (3)$$

The bearing capacity does not increase linearly with the width of the footing or overburden contrary to that obtained from Equation (2). This phenomenon is called the scale effect by de Beer [19, 20], who attributed this to the nonlinear shape of the soil failure envelope resulting in the secant measure of the friction angle, which decreases with mean effective confining stresses. With increasing confinement, dense and loose cohesionless soils have much less marked difference in peak angle of internal friction. This effect is more pronounced in geomaterials such as coal ash that suffer from progressive crushing. McDowell and Bolton [21] have provided additional data that support reduction in the peak angle of friction at the pile tip in the case of high overburden pressure and relative density.

Equation 2 may be expressed for a circular cone as

$$q_{ult} = S_q(\sigma'_{ov} N_q + 0.5 N_\gamma \gamma' B) \quad (4)$$

The empirical shape factor S_q is taken as 1.3 due to the circular shape of the penetrometer base.

For cone penetration bearing capacity, the factors N_q and N_γ may be grouped together. Therefore cone resistance may be rewritten as

$$q_c = \sigma'_{ov} N_{\gamma q} \quad (5)$$

Using a concept proposed by de Beer [19, 20], $N_{\gamma q}$ may be put forward as

$$N_{\gamma q} = \tan^2(\pi/4 + \phi'/2)\, e^{2\pi \tan \phi'} \quad (6)$$

Experimentally it is obtained as

$$N_{\gamma q} = q_c / S_q * \sigma'_{ov} \quad (7)$$

where q_c = the point resistance per unit area, S_q = the shape factor, conventionally taken as 1.3, which is not required in the relative dilatancy approach, and σ'_{ov} = the overburden pressure at the test level due to the weight of the ash. Some investigators have suggested modification in the bearing capacity factor $N_{\gamma q}$ for the cone apex angle (Cassidy and Houlsby [22]) and the roughness of the base contact surface (Meyerhof [23]). The use of a standard cone penetration device throughout the testing program allowed the authors to interpret the effect of cone apex angle and the roughness of the base contact surface as a common factor grouped in the ratio of experimental values of $N_{\gamma q}$ and $N_{\gamma q}(\phi)$ obtained from the angle of internal friction. Since ϕ varies as the state of stress, density, and material characteristics of the soil, the concept of stress dilatancy enunciated by Rowe [24], modified by de Josselin de Jong [25], and developed by Bolton [26] is utilized.

Bolton proposed the empirical equation

$$\phi_{peak} = \phi_{cr} + A I_r \quad (8)$$

where

$$I_r = RD(Q - \ln p') - r \quad (9)$$

where A is an empirical constant and has the value of 3 for axisymmetrical case; I_r is the relative dilatancy index; p' is the mean effective confining pressure in kPa; RD is relative density; and Q and r are empirical material fitting constants with values of 10 and 1, respectively, for clean silica sand. The dilatancy increases with increasing Q and decreases with increasing r (Salgado et al. [27]). Incorporating Billam's [28] triaxial test data, Bolton [26] suggested that progressive crushing suppresses dilatancy in the soils with weaker grains, i.e. limestone, anthracite, and chalk, which show Q values of 8, 7, and 5.5, respectively. The Ropar ash, which may be classified as ASTM class F ash, contains a substantial amount of crystalline fine silica grains, followed by alumina and the oxides of iron, calcium, and magnesium. It shows a Q as low as 7.7 (Singh [29], Trivedi and Sud [30]). This occurs mainly because of reduction of the critical mean confining pressure, beyond which increases in mean confining pressure for a relative density do not increase peak angle above the critical angle. Perkins and Madson [31] proposed to integrate this approach of progressive failure with the bearing capacity of shallow foundations on sand. This approach is presently modified and extended to meet the requirements of the cone penetration test on an ash fill.

Experimental Methods

The experimental methods consisted of chemical and physical analysis of ash procured from a thermal power plant at Ropar, Punjab, India. To serve a micromechanical purpose, the oven-dry ash sample was scanned by an electron microscope at × 1000. The wet chemical and X-ray diffraction analysis of incombustibles in the ash was conducted to find out the chemical and mineralogical composition. The grain size analysis of the dry ash sample was conducted by the mechanical sieve method. For the fraction passing the 75 μm sieve, a hydrometer method was employed separately.

In order to evaluate the cone penetration resistance of ash fill, this ash was deposited in loose lift of 150 mm in a trench of plan dimension of 1.5 m × 1.5 m (Fig. 1*a*). It was compacted by a precalibrated plate vibrator mounted on a flat rectangular plate (152 mm × 390 mm). The rating of the plate vibrator was 2950 rpm. A constant magnitude of vibration was required to achieve the desired relative density. The trench was filled up in layers maintaining constant density throughout. The density checks were applied at regular intervals using thin core cutter sampling and penetration of an 11-mm-diameter needle penetrometer under a constant pressure (Fig. 1*b*). After filling ash up to a desired level the static cone penetration test was initiated on the compacted ash.

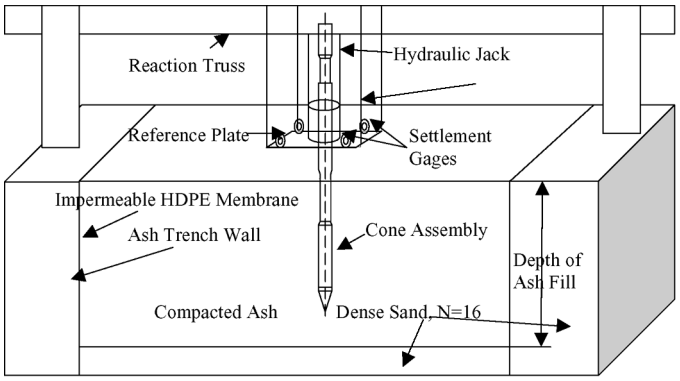

FIG. 1*a*—*Experimental setup for cone penetration test in ash fills.*

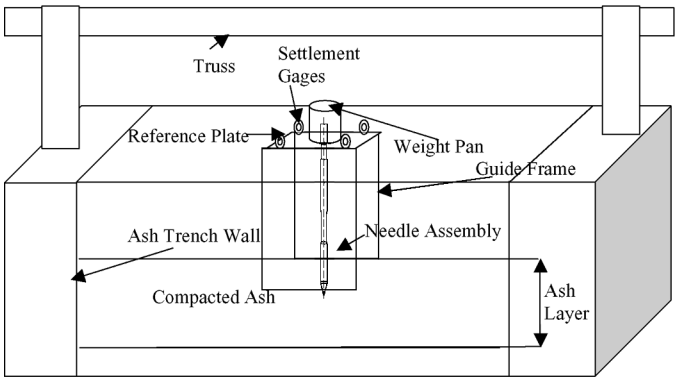

FIG. 1*b*—*Experimental setup for needle penetration test for density checks in ash fills.*

TABLE 2—*Water content for ash compacted at varying relative densities.*

RD (%)	Water Content (%)
51.6	34.85
77.4	36.95
80.8	38.05
85.5	39.57

The cone penetration assembly consisted of a slender metal rod driven into the ash fill with a controlled rate of penetration by a hydraulic jack and reaction system (Singh [32]). Dayal and Allen [33] observed an insignificant effect of rate of penetration on penetration resistance of cohesionless material (silica-70 sand). Since ash is a free-draining material with a high coefficient of permeability, pore water pressure during a slow rate of penetration (20 mm/s) at a low degree of saturation (less than 50 % in all the tests) would be negligible (see Table 2 for water content). The resistance to the penetration of the metal rod was measured at varying depths. Additionally, in situ density checks and laboratory shear box tests were also conducted. The penetration of the rod was monitored using precalibrated settlement gages of least count 0.01 mm. The force for the penetration of the cone and the sleeve was recorded with the help of a proving ring. The total assembly including hydraulic jack, proving ring, and cone was aligned with the help of a plumb bob to attain verticality. The cone penetration test was conducted using a cone (area of cone base, $A_c = 9.97\ cm^2$) with apex angle of 60° and removable friction sleeve (area of sleeve surface, $A_s = 148\ cm^2$). The extension rod was pressed in alignment into the ash fill at a rate of 20 mm/s to measure the cone tip force (Q_c) and the total force (Q_t). The cone with friction sleeve was pushed into the ash next to estimate total force (Q_t). The average values of point force and total force recorded from at least four tests at a common density and depth were used to calculate the cone tip resistance ($q_c = Q_c/A_c$) and frictional resistance ($q_f = (Q_t - Q_p)/A_s$).

Interpretation of Results

Characterization

The chemical analysis of Ropar ash used in this study indicates SiO_2 (57.5 %), Al_2O_3 (27.2 %), Fe_2O_3 (5.4 %), nonreactive CaO (3.1 %), MgO (0.4 %), soluble material (<1 %), and unburned carbon (~4 %) by weight. The mechanical properties of ash depend

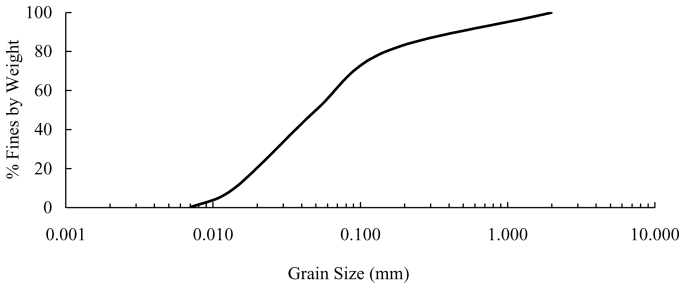

FIG. 2—*Grain size distribution of coal ash.*

on the grain size, shape, and distribution. Micrographic observations (Trivedi and Sud [30]) indicated the existence of the following constituents in Ropar ash:

- Siliceous aluminous particles (brownish glass spherules)
- Rounded porous grains (white sponge-like grains)
- Agglomerated glass spherules (reflecting)
- Magnetite (dark grays), hematite (red)
- Irregular porous grains of carbon (black)

Grain Size, Specific Gravity, and Void Ratio

Figure 2 shows the grain size analysis of coal ash. The ash consists of grain sizes corresponding to well-graded sandy silt. The maximum cone tip resistance on the Ropar ash ranges from 2000 to 6000 kPa at varying relative densities. Using Douglas and Olsen [34] charts for SCPT in natural soils, the range of particle sizes of coal ash is indicated to be clayey silt to silty clay while ash contains particle sizes in the range of coarse sand to silt with maximum frequency of particles in the range of fine sand to silt (Fig. 2). The reasons for this inconsistency are attributed to low specific gravity (1.98) of coal ash compared to natural soils (∼2.6). The maximum and the minimum void ratio of ash samples were found to be 1.52 and 0.78 respectively.

Density Checks on Compacted Ash Fill

A needle penetrometer designed by Sharma [35] was used to verify the relative density of compacted ash in the test trench (Fig. 1*b*). This consists of a graduated and smooth glass tube of 11 mm external diameter. The penetration of the needle penetrometer was calibrated at known relative densities. It was used as a probe to ascertain the density state of ash in the trench. A special device was fabricated to monitor the vertical movement of this probe. On the top of the probe a platform was attached so that a fixed weight could be placed on it. The ash was vibrated in a 3000 mL cylindrical vessel with an inside diameter of 150 mm under a surcharge of 248 N and at a frequency of 60 Hz. The relative density was interpreted from maximum and minimum density estimates obtained by the weight-volume relationship at vibration intervals of 30 s each. The penetration of the probe under a constant pressure was allowed into the ash at varying relative densities. A plot, prepared for the verification of relative density with depth of penetration of the needle is shown in Fig. 3. However, for low relative densities the estimates of density were based solely upon the weight-volume relationship.

Cone Tip Resistance and Frictional Resistance

The cone resistance is controlled by in situ relative density, vertical and horizontal effective stress, and compressibility of the fill.

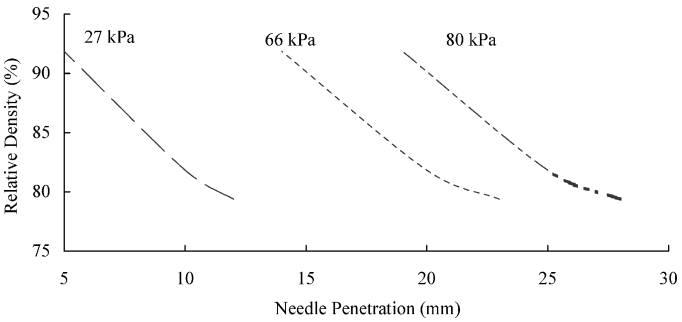

FIG. 3—*Relative density versus needle penetration for coal ash.*

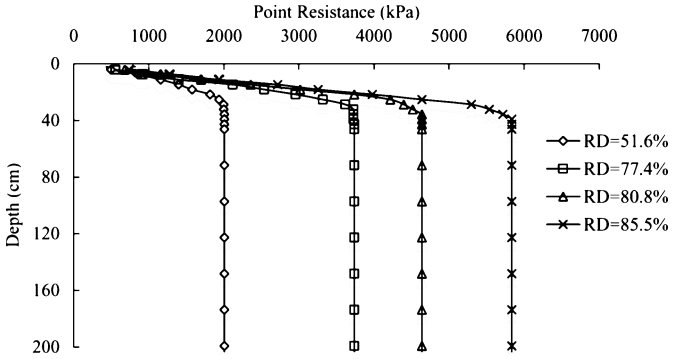

FIG. 4*a*—*Variation of cone resistance with depth of penetration for coal ash.*

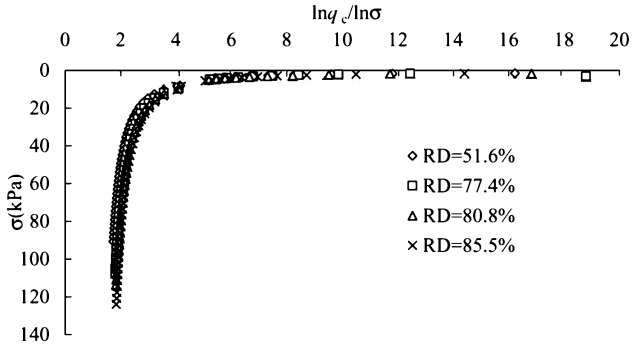

FIG. 4*b*—$\ln q_c / \ln \sigma$ *versus* σ_{ov} *for coal ash.*

The cone tip resistance q_c in ash increased with increasing relative density and depth of the deposit as shown in Fig. 4*a*. In Fig. 4*b* the effect of overburden (σ_{ov}) on cone tip resistance (q_c) at varying relative densities has been drawn (Singh [32]). The large scatter at shallow depths signifies unstructured response at low confining pressures. The relationship between the overburden and the cone resistance at varying relative densities (Fig. 4*b*) followed an empirical law as per Eq 10

$$(\ln q_c)/\ln \sigma = \zeta\{\sigma\}^{\psi} \tag{10}$$

where ζ and ψ are fitting parameters that vary with relative density (Table 3) with a satisfactory value of coefficient of regression (R^2). The cone resistance q_c and overburden pressure σ_{ov} are expressed in kPa.

The cone resistance q_c was found to become constant at a certain depth. The depth at which the peak resistance is reached keeps increasing with the increase in relative density, similar to cohesionless soils. The friction ratio, defined as a ratio of sleeve and cone

TABLE 3—*Fitting parameters ζ and ψ for ash at varying relative densities.*

RD (%)	ζ	ψ	R^2
51.6	11.634	−0.4588	0.9465
77.4	11.550	−0.4401	0.9470
80.8	11.500	−0.4258	0.9537
85.5	11.234	−0.4035	0.9639

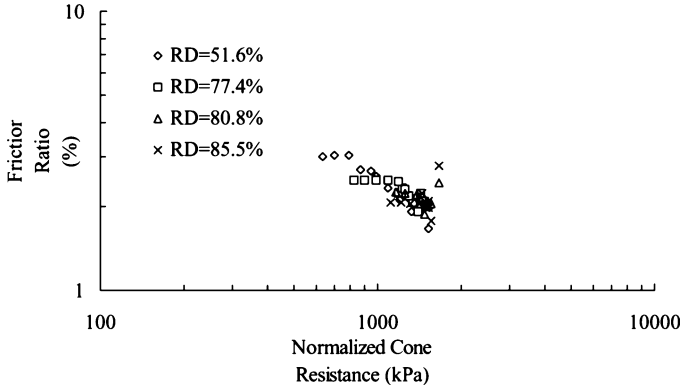

FIG. 4*c*—*Normalized cone resistance versus friction ratio of coal ash.*

resistance in percentages, decreased with increase in normalized point resistance at low relative densities, while the trend reversed at high relative densities (Fig. 4*c*). The normalized cone resistance is defined as a ratio of difference of cone resistance and overburden pressure to overburden pressure. A low friction ratio (2–3 %) was observed for coal ash, similar to the value cited by Schmertmann [7] for clayey silt, silty sands, and silts.

Angle of Shearing Resistance

The peak effective angle of shearing resistance is based on the knowledge of relative density (*RD*) and the gradation characteristics. A series of shear tests conducted on ash samples obtained from compacted fill indicates that shear strength is derived mainly from frictional properties. Hence coal ash is treated as a perfectly frictional material with a curved failure envelope [29] in a triaxial shear test on the various ashes procured from the Ropar thermal plant. The peak angle of internal friction is used as an average of various tests corresponding to a relative density (*RD*) and a mean effective confining pressure (p') in kPa. The critical state friction angle was obtained by shearing an ash sample to axial strains in excess of 25–30 %. The value of Q for coal ash is found to be 7.7 (Trivedi and Sud [30]). The critical state friction angle for coal ash, a morphological mineralogical parameter, was observed to be 30° for Ropar ash. Therefore, as overburden increases, the peak frictional strength of ash corresponding to a relative density may be interpreted from Eq 11 as

$$Q.RD - r = 0.33(\phi'_p - \phi_c) + RD.\ln(p') \tag{11}$$

where ϕ_p and ϕ_c are peak and critical angles of friction, and Q and r are material fitting parameters for coal ash.

The coal ashes act as a perfectly frictional material in the shear test [1,29]. The angle of internal friction obtained from Eq (11) is plotted with overburden (Fig. 5). The extent of conservative estimates of ϕ' is presented as a function of relative density and mean effective confining pressure.

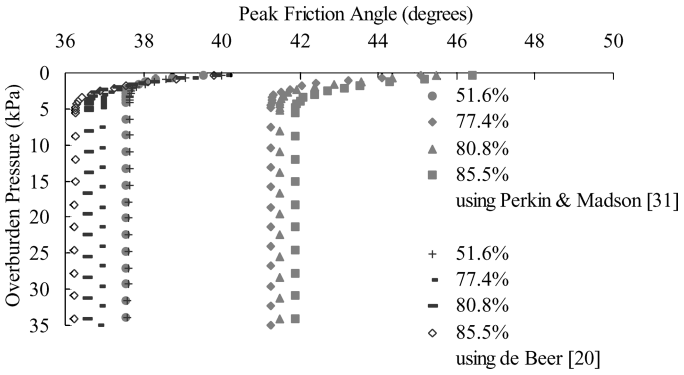

FIG. 5—*Variation of peak friction angle with overburden and relative density for coal ash.*

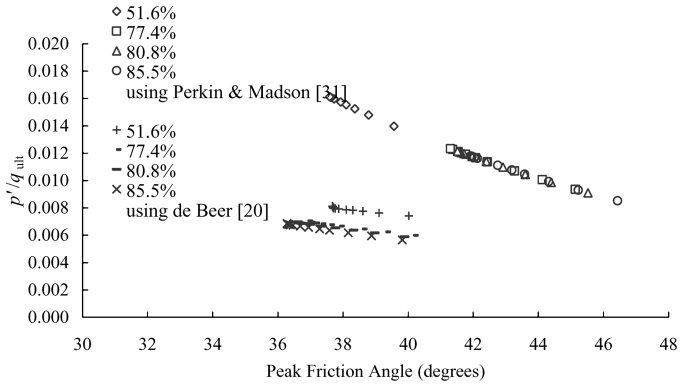

FIG. 6*a*—p'/q_{ult} *in axisymmetrical case versus peak friction angle at varying relative densities.*

The Bearing Capacity Factor

The experimental values of $N_{\gamma q}$ are compared with the values of $N_{\gamma q}(\phi)$ obtained from angle of internal friction using mean confining pressure as a function of ultimate load in cone penetration. Overburden pressure has been plotted assuming the fill to be semi-infinite and of uniform density resulting in constant penetration resistance to the cone below a depth of 2 m. The ratio of experimental (as per Eq 7) and theoretical (as per Eq 6) $N_{\gamma q}$ tends to converge to a constant value at a high overburden pressure for dense ash, thereby signifying a possibility of crushing. Figure 6*a* shows the relationship of effective mean confining pressure (p') with peak friction angle, taking into account the progressive failure. The expression suggested by de Beer [20] points towards a conservative estimate of p' owing to the overestimation of the effect of overburden. For the axisymmetrical case, de Beer [20] suggested that

$$p'/q_{ult} = 0.08 * (1 + 3\sigma'_v/q_{ult})(1 - \sin\phi')/4 \tag{12}$$

where q_{ult} is the ultimate bearing capacity of a footing; in the present case it is cone resistance q_c, and σ'_v is the effective overburden pressure.

Perkins and Madson [31] proposed an expression on the basis of nonlinear limit plastic analysis that has an advantage of consideration of a slip failure corresponding to a mean confining pressure and friction angle irrespective of overburden. For the axisymmetrical case,

$$p'/q_{ult} = 0.08 * 3.1\exp(-0.073 * \phi') \tag{13}$$

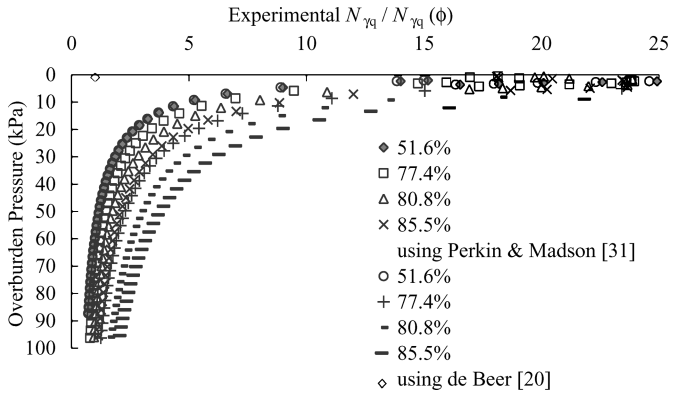

FIG. 6*b*—*Ratio of experimental and theoretical bearing capacity factor at varying relative densities versus overburden pressure.*

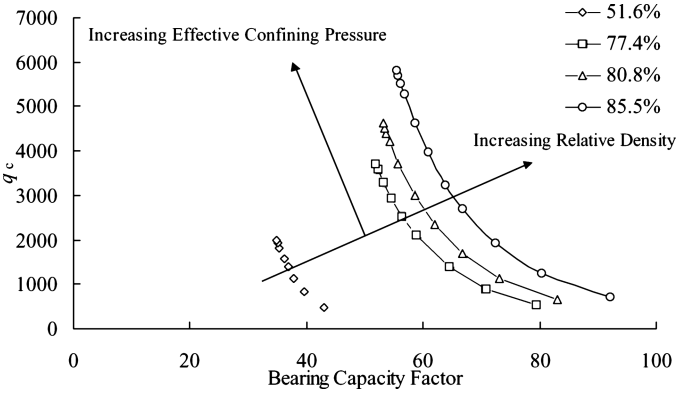

FIG. 7—*Variation of bearing capacity factor with cone resistance at varying relative densities.*

where q_{ult} is the ultimate bearing capacity of a footing; in the present case it is substituted by cone resistance q_c.

Figure 6*b* shows comparison of the ratio $N_{\gamma q}$ obtained experimentally using Eq (7) and $N_{\gamma q}$ obtained using the proposals of Perkins and Madson [31] and of de Beer [20]. Considerable gains in understanding may be achieved by analyzing the trend in the ratio of experimental $N_{\gamma q}/N_{\gamma q}(\phi)$ in Fig. 6*b*. The maximum value of experimental $N_{\gamma q}/N_{\gamma q}(\phi)$ at a relative density and overburden indicates the uncertainty of confinement at shallow depths, while convergences indicate arrival at a critical state or of crushing.

Bearing Capacity

The design of shallow foundations is often based on considerations of stability and deformation. Stability is usually evaluated using the concept of bearing capacity. An estimate of the ultimate bearing capacity of shallow foundations (q_{ult}) on cohesionless material (Meyerhof [36]), using the cone penetration test result, has been based upon empirical depth and shape factors:

$$q_{ult} = q_c * (B/12.2) * (1 + D/B) \tag{14}$$

where D is depth and B is width of the foundation in metres. Equation 14 provides a conservative estimate of the bearing capacity of ash fill.

With the help of the present approach, the bearing capacity can be evaluated by directly interpreting the bearing capacity factor ($N_{\gamma q}$) from the knowledge of relative density and cone resistance (Fig. 7). The increase in effective confining pressure increased the cone penetration resistance to a maximum but decreased the bearing capacity factor ($N_{\gamma q}$) at a constant relative density. The ultimate bearing capacity of a shallow foundation on ash fill may be obtained using Eq 15

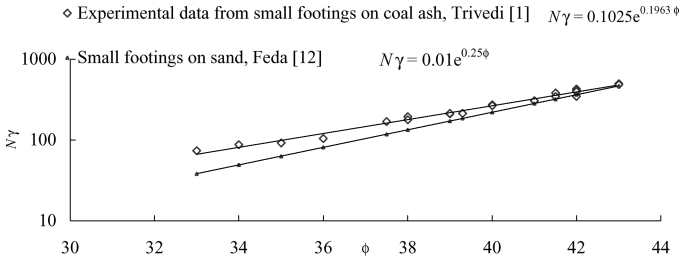

FIG. 8—*Empirical bearing capacity factor for coal ash.*

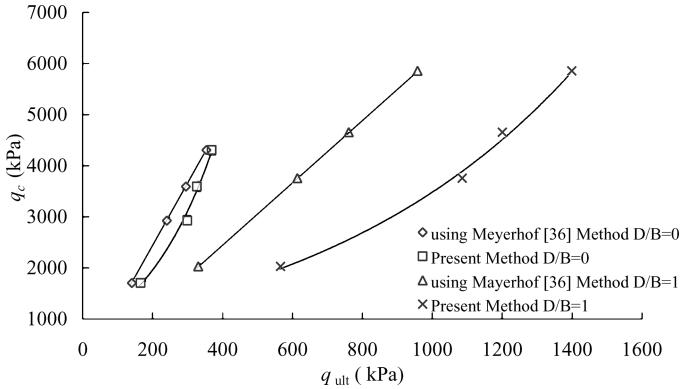

FIG. 9*a*—*Comparison of ultimate bearing capacity evaluated from cone resistance of coal ash.*

$$q_{ult} = 0.5 * B * \gamma * N_{\gamma q} \tag{15}$$

where the empirical bearing capacity parameter $N_{\gamma q}$ is proposed by the authors for the Ropar coal ash (Fig. 7). B is the footing width in metres and q_c is averaged over the depth ($D = B$) below the footing.

The bearing capacity of a square (0.09 m^2) surface footing on ash fill is compared with that obtained from N_γ proposed by Trivedi [1]. On the basis of a large number of small footing tests on Ropar ash, Trivedi [1] proposed an empirical relation (Eq 16) for evaluation of the bearing capacity of ash fills using the empirical bearing capacity factor (N_γ) and shape factor ($S_\gamma = 0.6$, for square footings). The variation of empirical bearing capacity factor (N_γ) with peak friction angle is indicated in Fig. 8. The N_γ values obtained by Feda [12] on sand are compared with the values obtained by Trivedi [1] on coal ash, using similar tests on small footings (Fig. 8).

$$N_\gamma = 0.1025 * e^{0.1963\phi'} \tag{16}$$

where N_γ is the bearing capacity factor obtained from plate load test data of Trivedi [1] on Ropar coal ash. The value of N_γ from Eq 16 as a multiple of shape factor is substituted for $N_{\gamma q}$ in Eq 15 to obtain the ultimate bearing capacity of ash fill corresponding to a peak friction angle.

Figure 9*a* shows a comparison of the bearing capacity of ash fill using the Meyerhof [36] method and the method proposed in the present study. The bearing capacity factor obtained from the plate load test data of Trivedi [1] was used to provide validation of the proposed method. The ultimate bearing capacity of ash fill was observed to fall between the estimates of the critical and the

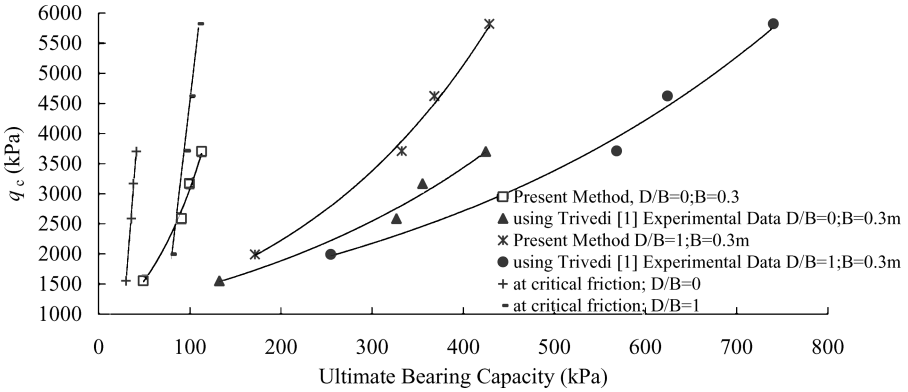

FIG. 9*b*—*Ultimate bearing capacity evaluated from critical, dilatant, and peak friction angles.*

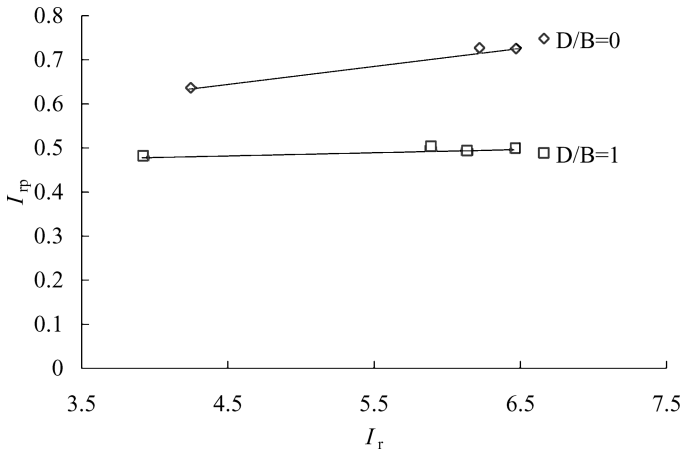

FIG. 10—*Extent of progressive failure in coal ash.*

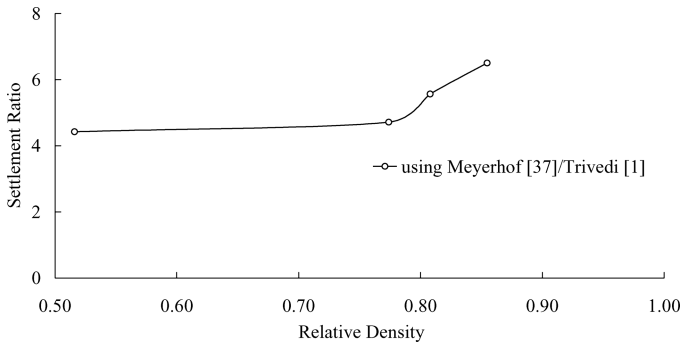

FIG. 11—*Variation of settlement ratio with relative density for coal ash.*

peak friction angles. Figure 9*b* indicates that the bearing capacity of ash fill evaluated by the present method is always lower than that obtained by the use of the peak friction angle. The advantage of using the present method is doing away with empirical depth and shape factors that seem to be more speculative for large sizes of footing. Figure 10 shows the variation in the index of progressive failure (I_{rp}) with the relative dilatancy index for a surface and an embedded footing. The index of progressive failure is defined as

$$I_{rp} = \left[q_{ult\,(at\,\phi' peak)} - q_{ult\,(from\,cone\,penetration\,test)}\right] / \left[q_{ult\,(at\,\phi' peak)} - q_{ult\,(at\,\phi\,critical)}\right] \quad (17)$$

If I_{rp} takes a value of unity, it implies that the ultimate bearing capacity of ash fill is governed by the critical friction angle, while a value of zero indicates that the peak angle of friction is fully mobilized. The occurrence of a relatively high value of the factor $Q - \ln p'$ at peak cone resistance in ash fills leads to higher values of relative dilatancy index among ashes.

Settlements

The settlements of Ropar ash of the same grain size and characteristics were determined from the data of the plate load test conducted by Trivedi [1] (at $D/B = 0$ and $B = 0.6$ m) and were compared with the settlement of a footing of similar dimension utilizing the cone penetration test data for coal ash.

Meyerhof [37] suggested a simple method to estimate settlement (S_c) of a footing on sand directly from the cone penetration resistance as

$$S_c(\text{sand}) = \Delta p B / 2 q_c \quad (18)$$

where Δp = net foundation pressure. The cone resistance (q_c) is taken as the average over a depth equal to the width of the footing (B).

The evaluation of settlement using the Meyerhof [37] method at different densities shows a much higher settlement using the cone penetration data than by the plate load test (Trivedi [1] and Leonards and Bailey [9]). The settlement ratio (defined as a ratio of the settlement of ash using Eq 18 and the settlement computed from the plate load test data of Trivedi [1]) of coal ash increases with an increase in relative density (Fig. 11).

Utilizing the plate load test data of Trivedi [1] for Ropar ash compacted at different relative densities, it is proposed to modify Meyerhof's equation to

$$S_c(\text{coal ash}) = \Delta p B / [(4.8 * RD + 1.75) 2 q_c] \quad (19)$$

Using the knowledge of cone penetration resistance, relative density, net foundation pressure, and width of footing, the settlement of an ash fill may be computed directly using Eq 19. The main source of difference in the settlement computed from Eq 18 and the cone penetration test data lies in the estimate of deformation modulus of deposits. Equation 19 takes care of the increase in the deformation modulus due to the material characteristics and increase in the relative density of coal ash.

Conclusions

The static cone penetration test is an excellent tool for the assessment of the geotechnical design parameters of the coal ash

deposit. The friction ratios in coal ash are higher than those of soils of similar gradation because of the morphology of the ash particles. The knowledge of relative density, peak friction angle, and mean confining pressure are used in relation to relative dilatancy of the ash to correlate shear strength with penetration resistance. The bearing capacity of shallow foundations on ash fill, estimated using conventional methods, leads to a conservative estimate because of the empirical factors that are derived mainly for sandy soils. The use of the relative dilatancy index in prediction of ultimate bearing capacity in relation to penetration resistance was validated using data from the plate load test on coal ash. It is proposed to use the bearing capacity factor as per the magnitude of cone penetration and relative density of ash fill (Fig. 7). The settlement of ash fill obtained using the conventional method was found to be significantly higher when compared with the plate load test results. A modified empirical relation is proposed on the basis of cone penetration test results to obtain the settlement characteristics of the ash fill.

Acknowledgments

The study presented here is based on the data presented in doctoral and master level thesis work on coal ash at TIET, Patiala and the analytical work of the authors at Delhi College of Engineering, Delhi. However, opinions, findings and conclusions expressed herein are those of the authors and pertain only to the observed data set and do not necessarily reflect the behavior of all types of coal ashes. The suggestions of Professor Steven W. Perkins, Department of Civil Engineering, Montana State University, Bozeman, Montana, and his useful insight into the application of the relative dilatancy approach to the bearing capacity are greatly appreciated. The assistance of numerous fellow workers in procurement of material and sampling is thankfully acknowledged.

References

[1] Trivedi, A., "Engineering Behavior of Coal Ash," Ph.D. Thesis, Department of Civil Engineering, Thapar Institute of Engineering and Technology, Patiala, India, 1999.

[2] Lunne, T., Robertson, P. K., and Powell, J. J. M., *Cone Penetration Testing in Geotechnical Practice*, Blackie Academic and Professional Publications, London, 1997.

[3] Bellotti, R., Bizzi, G., and Ghionna, V., "Design Construction and Use of a Calibration Chamber," *2nd European Symposium on Penetration Testing*, Amsterdam, Vol. 2, 1982, pp. 439–446.

[4] Cunningham, J. A., Lukas, R. G., and Andreson, T. C., "Improvement of Fly Ash and Stage—A Case Study," *Proceedings, Conference on Geotechnical Practice for Disposal of Solid Waste Materials*, American Society of Civil Engineers, Ann Arbor, MI, 1977, pp. 227–245.

[5] Toth, P. S., Chan, H. T., and Crag, C. B., "Coal Ash as Structural Fill With Reference to Ontario Experience," *Canadian Geotechnical Journal*, Vol. 25, 1988, pp. 594–704.

[6] Seals, R. K., Moulton, L. K., and Kinder, D. L., "In Situ Testing of a Compacted Fly Ash Fill," *Proceedings, Conference on Geotechnical Practice for Disposal of Solid Waste Materials*, American Society of Civil Engineers, Ann Arbor, MI, 1977, pp. 493–516.

[7] Schmertmann, J. H., "Guidelines for Cone Penetration Test, Performance and Design," US Federal Highway Administration, Washington, DC, Report FHWATS-78-209, 1978, p. 145.

[8] Begemann, H. K. S., Ph., "The Friction Jacket Cone as an Aid in Determining the Soil Profile," *Proceedings, 6th International Conference on Soil Mechanics and Foundation Engineering*, Montreal, Vol. 1, 1965, pp. 17–20.

[9] Leonards, G. A. and Bailey, B., "Pulverized Coal Ash as Structural Fill," *Journal of Geotechnical Engineering*, American Society of Civil Engineers, Vol. 108, GT4, 1982, pp. 517–531.

[10] Prandtl, L., Über die Harte Plastischer Korper (in German). Nachr, Kgl. Ges Wiss Gottingen Math. Phys. K. O. I. Berlin, 1920, pp. 74–85.

[11] Reisner, H., "Zum Erddrulk Problem," (in German), *Proceedings, 1st International Conference on Applied Mechanics*, Delft, The Netherlands, 1924, pp. 295–311.

[12] Feda, J., "Research on Bearing Capacity of Loose Soil," *Proceedings, 5th International Conference on Soil Mechanics and Foundation Engineering*, Paris, Vol. 1, 1961, pp. 635–642.

[13] Meyerhof, G. G., "Some Recent Research on Bearing Capacity of Foundations," *Canadian Geotechnical Journal*, Vol. 1, No. 1, 1963, pp. 16–26.

[14] Meyerhof, G. G., "Shallow Foundations," *Journal of Soil Mechanics and Foundation Division*, ASCE, SM2, Vol. 91, 1965, pp. 21–31.

[15] Brinch Hasen, J., "A Revised and Extended Formula for Bearing Capacity," Bulletin No. 28, Danish Technical Institute, Copenhagen, 1970, pp. 5–11.

[16] Vesiĉ, A. S., "Analysis of Ultimate Loads of Shallow Foundations," *Journal of Soil Mechanics and Foundation Division*, American Society of Civil Engineers, Vol. 99, No. SM-1, 1973, pp. 45–69.

[17] Chen, W. F., *Limit Analysis and Soil Plasticity*, Elsevier, Amsterdam, 1975.

[18] Zadroga, B., "Bearing Capacity of Shallow Foundations on Noncohesive Soils," *Journal of Geotechnical Engineering*, American Society of Civil Engineers, Vol. 120, No. 11, 1994, pp. 1991–2008.

[19] de Beer, E. E., "The Scale Effect in the Transposition of the Results of Deep Sounding Tests on the Ultimate Bearing Capacity of Piles and Cassion Foundations," *Geotechnique*, Vol. 8, No. 1, 1963, pp. 39–75.

[20] de Beer, E. E., "Bearing Capacity and Settlement of Shallow Foundations on Sand," *Proceedings, Symposium on Bearing Capacity and Settlement of Foundations*, Duke University, Durham, NC, 1965, pp. 15–33.

[21] Mcdowell, G. R. and Bolton, M. D., "Effect of Particle Size Distribution on Pile Tip Resistance in Calcareous Sand in the Geotechnical Centrifuge," *Granular Matter*, Vol. 2, No. 4, 2000, pp. 179–187.

[22] Cassidy, M. J. and Houlsby, G. T., "Vertical Bearing Capacity Factors for Conical Footings on Sand," *Geotechnique*, Vol. 52, No. 9, 2002, pp. 687–692.

[23] Meyerhof, C. G., "The Ultimate Bearing Capacity of Foundations," *Geotechnique*, Vol. 2, No. 4, 1951, pp. 301–332.

[24] Rowe, P. W., "The Stress Dilatancy Relation for Static Equilibrium of an Assembly of Particles in Contact," *Proceedings, Royal Society*, London, A269, 1962, pp. 500–527.

[25] de Josselin de Jong, G., "Rowe's Stress Dilatancy Relation Based on Friction," *Geotechnique*, Vol. 26, No. 3, 1976, pp. 527–534.

[26] Bolton, M. D., "The Strength and Dilatancy of Sands," *Geotechnique*, Vol. 36, No. 1, 1986, pp. 65–78.

[27] Salgado, R., Bandini, P., and Karim, A., "Shear Strength and Stiffness of Silty Sand," *Journal of Geotechnical and*

Geoenvironmental Engineering, American Society of Civil Engineers, Vol. 126, No. 5, 2000, pp. 551–562.

[28] Billam, J., "Some Aspects of the Behaviour of Granular Material at High Pressures," *Stress Strain Behaviour of Soils*, R. H. V. Parry, Ed., Foulis, London, 1972, pp. 69–80.

[29] Singh, R., "Small Strain Stiffness and Strength Characteristics of Ash," M. E. Thesis, Department of Civil Engineering, Thapar Institute of Engineering and Technology, Patiala, India, 2002.

[30] Trivedi, A. and Sud, V. K., "Grain Characteristics and Engineering Properties of Coal Ash," *Granular Matter*, Vol. 4, No. 3, 2002, pp. 93–101.

[31] Perkins, S. W. and Madson, C. R., "Bearing Capacity of Shallow Foundations on Sand: A Relative Density Approach," *Journal of Geotechnical and Geoenvironmental Engineering*, American Society of Civil Engineers, Vol. 126, No. 6, 2000, pp. 521–529.

[32] Singh, C., "Static Cone Penetration Resistance of Ash Fill," M. E. Thesis, Department of Civil Engineering, Thapar Institute of Engineering and Technology, Patiala, India, 2001.

[33] Dayal, U. and Allen, J. H., "Effect of Penetration Rate on the Strength of Remolded Clay and Sand Samples," *Canadian Geotechnical Journal*, Vol. 12, No. 3, 1975, pp. 336–348.

[34] Douglas, B. J. and Olsen, R. S., "Soil Classification Using Electric Cone Penetrometer: Cone Penetration Testing and Experience," *Proceedings, American Society of Civil Engineers National Convention*, St. Louis, MO, 1981, pp. 209–227.

[35] Sharma, M., "Load Bearing Characteristics of Ash Fill," M. E. Thesis, Department of Civil Engineering, Thapar Institute of Engineering and Technology, Patiala, India, 1999.

[36] Meyerhof, C. G., "Penetration Tests and Bearing Capacity of Cohesionless Soils,"*Journal of Soil Mechanics and Foundation Division*, American Society of Civil Engineers, Vol. 82, SM1, 1956, pp. 1–19.

[37] Meyerhof, G. G., "Penetration Testing Outside Europe," General Report European Symposium on Penetration Testing, Stockholm, Vol. 2.1, 1974, p. 40–8.

[38] Dayal, U., Shukla, S., and Sinha, R., "Geotechnical Investigations for Ash Dikes," *Fly Ash Disposal & Deposition*, Narosa, New Delhi, 1999, pp. 22–31.

[39] Sood, V. K., Trivedi, A., and Dhillon, G. S., "Report on Dike Construction for the Disposal of Fly Ash at Ropar," Department of Civil Engineering, Thapar Institute of Engineering and Technology, submitted to PSEB, Patiala, India, 1993.

APPENDIX: *List of Notations*

ϕ'	effective friction angle (degrees)	N_c, N_q, N_γ	bearing capacity factors for shallow footing
σ	overburden pressure (kPa)	$N_{\gamma q}$	bearing capacity factor from cone penetration test
γ'	buoyant unit weight (kNm^{-3})	$N_{\gamma q}(\phi)$	bearing capacity factor calculated from friction angle
ϕ_{cr}	critical state friction angle (degrees)	NCR	normalized cone resistance
Δp	net foundation pressure (kPa)	p'	mean confining pressure (kPa)
ϕ_{peak}	peak friction angle (degrees)	Q, r	empirical material constants
σ_{ov}	overburden pressure (kPa)	q'	effective overburden pressure at foundation level (kPa)
σ_{vp}	effective vertical stress below foundation where its peak occurs (kPa)	q_c	point resistance per unit area at cone tip (kPa)
		Q_c	point force
Δz	thickness of layer (m)	q_c	Q_c/A_c
A	an empirical constant; 3.0 for axisymmetrical case	q_s	frictional resistance
A_c	area of cone base, 9.97 cm^2	Q_t	total force required for penetration of cone and sleeve
A_s	area of sleeve surface, 148 cm^2	q_{ult}	ultimate bearing capacity
B, D	width, depth of footing (m)	RD	relative density
c'	effective cohesion (kPa)	$RD1,2,3,4$	relative density of 51.6, 77.4, 80.8, and 85.5 %, respectively
I_r	relative dilatancy index		
I_{rp}	index of progressive failure	S_c	settlement of footing on coal ash (mm)
I_z	influence factor	S_q	empirical shape factor
N	SPT number	ζ and ψ	fitting parameters for varying relative densities